

Cosmological analysis of the satellite galaxy distribution

M.A. Gómez-Flechoso, L. Benjouali, R. Domínguez Tenreiro

Abstract There exists galaxy systems in the Local Universe formed by satellite dwarf galaxies orbiting a main one. The knowledge of the satellite distribution and their characteristics gives information about the formation and assembly processes of the galaxies in the Universe. In this paper, we analyze the satellite distribution around disk galaxies in cosmological hydrodynamical simulations, both in three-dimensions (3D) and in projection along random directions, mimicking observational strategies. It has been found that, at short 3D distances, the satellite orbits in rich systems (that is, systems with high number of satellites) have on average a polar distribution. The orbital distribution in projection at short distances between the satellite and its host shows a lack (excess) of minor-axis alignments for poor (rich) systems. Therefore, the alignments onto a virtual sky would appear mostly isotropic (i.e., no-preferred major or minor axis alignments), or even planar (i.e., major-axis alignments), depending the selected sample, in consistency with most observational analyses.

1 Introduction

In the hierarchical scenario for galaxy formation, main galaxies were formed by aggregation of smaller sub-structures. The present-day systems of primary galaxies and their satellites (i.e., the surviving ones) could provides information about these assembling processes. For example, the satellite distribution relative to the hosts at

M.A. Gómez-Flechoso
Univ. Autónoma de Madrid, 28049 Cantoblanco (Madrid), e-mail: mangeles.gomez@uam.es

L. Benjouali
Univ. Autónoma de Madrid, 28049 Cantoblanco (Madrid), e-mail: latifa.benjouali@uam.es

R. Domínguez Tenreiro
Univ. Autónoma de Madrid, 28049 Cantoblanco (Madrid) e-mail: rosa.dominguez@uam.es

$z = 0$ gives us information about the anisotropy and the time scales of the accretion process, and the structure of the galaxy halo.

There is not observational agreement about satellite distributions. In the Local Group, satellites seem to follow a polar distribution. The closest dwarfs of the Milky Way form Great Circles roughly perpendicular to the Galactic Plane (Lynden-Bell 1982; Majewski 1994; Kroupa, Theis & Boldy 2005; Zentner et al. 2005), and a similar behavior is observed in the M31 satellite distribution (Koch & Grebel 2006). In external galaxies, Holmberg (1969) analyzed the satellite distribution in populated disk-galaxy systems for projected radial distances from the primary $d_p < 50$ kpc, finding a depletion of satellites within projected angles 30° of the primary disk (i.e., the Holmberg effect, a polar alignment in projection). However, Valtonen, Teerikorpi, & Argue (1978) have found a planar alignment. Zaritsky et al. (1997) have analyzed a sample of 115 satellites of isolated spirals finding no evidence of polar alignment for those placed at $d_p < 200$ kpc, but a visual appearance of planar alignment, while for those verifying $d_p > 250$ kpc, a significant polar signal is found. The number of those for which $d_p < 50$ kpc is too low to confirm Holmberg's findings. Most recent analysis of large redshift surveys also reach different conclusions. Some of them find planar alignments, in apparent disagreement with the Milky Way satellite anisotropic configuration. Brainerd (2005), using r' band photometric data from the SDSS DR3, analyzed samples of satellites of isolated primaries (mainly spirals), and she finds planar alignment for satellites with $d_p < 100$ kpc, while for those on larger scales ($250 < d_p < 500$ kpc) their distribution is consistent with isotropy. However, polar alignments have been recently reported by Bailin et al. (2007) in the SDSS DR5, applying very careful isolation criteria for the mains. Still other authors find alignments consistent with isotropy in the projected satellite distribution, as Azzaro et al. (2007) for a large sample of blue main galaxies from the SDSS DR4.

Other authors use numerical simulations to investigate galaxy configurations. Agustsson & Brainerd (2006), in their analysis of GIF N-body simulations of Λ CDM universes combined with semi-analytic prescriptions for galaxy formation, find that, in projection, satellites are preferentially located close to the major axes of the projected host *halo*. To compare these results with observations, we need to know how disks are oriented relative to the inertia axes of the haloes where they are embedded, however this information is not provided by GIF simulations. Only when particular orientations are assumed, the results above could imply an anisotropy of the satellites relative to their host *galaxies*, but the anisotropy will reach beyond two virial radii. Similar results have been obtained by Sales et al. (2007) in their analysis of the Millenium simulation. Other authors have focused on the analysis of Milky Way-like host-satellite systems (i.e., with 10 - 12 luminous satellites per host, see Zentner et al. 2005; Kang et al. 2005; Libeskind et al. 2005, 2007). They find that these satellite systems are generally flattened into nearly planar ellipsoids aligned with the longest axis of the triaxial host dark matter halo, therefore the consistency with Milky Way data would demand that the longest axes is roughly perpendicular to the galaxy disks and, to prove it, hydrodynamical simulations are needed.

Libeskind et al. (2007) have found such configurations in 2 of the 3 populated disk-satellite systems identified in their hydrodynamical simulations.

None of these studies have used *samples* of disk-like galaxies (DLOs) formed in fully-consistent cosmological hydrodynamical simulations, and, except for Libeskind et al. (2007), none used DLOs at all. DLO samples allow to analyze satellite configurations in three dimensions (3D) and in projection on the sky. In this work we present an analysis of the 3D orbital distribution of a sample of virtual satellites around DLOs and we compare this distribution with that inferred from their virtual projected images.

2 Methodology

We have used the DEVA numerical code, a Lagrangian SPH-AP3M code, and its OpenMP parallelized version, p-DEVA, to run hydrodynamical numerical cosmological simulations. Particular attention has been paid to hold the conservation laws (energy, entropy and angular momentum) as accurately as possible (see Serna, Domínguez-Tenreiro, & Sáiz 2003 for details on the simulation code). Several sets of simulations have been run: i), using DEVA in a periodic box of 10 Mpc side, with 64^3 dark matter (DM) particles and 64^3 baryonic particles and the following sets of cosmological parameters: $(\Omega_m, \Omega_b, h) = (0.35, 0.06, 0.65)$ or $(0.3, 0.04, 0.7)$; and ii), using P-DEVA with a periodic box of 20 Mpc side, 128^3 DM particle, 128^3 baryonic particles and $(\Omega_m, \Omega_b, h) = (0.3, 0.04, 0.7)$. Galaxy-like objects of different morphologies are generated in all simulations. Objects with an extended, massive rotating disk and a central, dynamically relaxed, spheroidal component or bulge, embedded both in a dark halo, have been identified as DLOs. Structural and dynamical properties of the DLOs are consistent with observations (see Sáiz et al. 2001). We have selected a first sample of more than 200 DLOs with baryonic mass smaller than $3 \times 10^{10} M_\odot$ and having a satellite system. To make realistic comparisons with observational data, we have adopted the same isolation criteria as Brainerd (2005) to select in our simulations isolated DLOs and their satellite systems. The total sample (T sample) fulfilling the isolation criteria includes 45 DLOs and 553 satellites (within a distance of $r = 1.6$ Mpc from their hosts). To build up their samples, some observers (quoted in §1) applied a selection criterion, namely the non-binarity condition which, in terms of the mass, requires that each satellite must be at least 6.25 times less massive than its host (otherwise the system is termed binary). By applying the non-binarity selection criterion to the DLO-satellite systems in the T sample, a subsample that contains 14 DLOs and 141 satellites (within a distance of $r = 1.6$ Mpc from their hosts) is built. We will refer to it as the NB (non-binary) sample.

To mimic observations we have projected our DLO-satellite systems along random directions, and computed the projected distance, d_p of each satellite relative to its host. Doing this, the actual number of satellites with $d_p < 500$ kpc in the T and NB samples is 189 and 43, for 45 and 14 DLOs, respectively.

To understand the differences between the various analyses of the observational surveys, it is worth recalling that some of the samples, as Holmberg's, Milky Way and M31 samples, comprise systems with high average number of satellites per host, while all the others (see §1) contain isolated hosts with a lower number of satellites. To find out whether these differences could affect the satellite distribution or not, we have classified our systems as rich (those with more than 3 satellites seen in projection) or poor (3 or less than 3 satellites seen in projection). Then, we split both the T and NB samples in rich and poor subsamples and we analyze the R (rich systems of the T sample), the P (poor systems of the T sample) and the P.NB (poor systems of the NB sample) systems.

3 Results and Conclusions

We analyzed 3D trajectories of satellites relative to the host disk at $z = 0$. To explain the results, we need to define the disk total angular momentum of a given host, \mathbf{J}_D ; the orbital angular momentum of a satellite relative to the disk, \mathbf{J}_S , and the angle, θ_J , between them. The satellite has a *polar trajectory* if $45^\circ < \theta_J < 135^\circ$. The 3D position of a satellite with respect to the host disk can be measured using the angle between the satellite position vector and the plane of the disk. A satellite is located in the *equatorial region* when this position angle takes values between -45° and 45° ; otherwise, the satellite is in the *polar cone*. As satellites travel all along the orbits, a satellite in a polar orbit could be either in the equatorial region or in the polar cone. Average θ_J values are displayed in Figure 1 as a function of the 3D distance between the satellite and the host (a range $0^\circ < \theta_J < 90^\circ$ has been used, and for angles greater than 90° we plot $180^\circ - \theta_J$). This figure gives valuable information on 3D orbital distribution of satellites relative to the hosts. At larger distances from the host (say, $r > 100$ kpc), all the samples present an isotropic distribution. Thus, the averaged percentage of polar orbits for isotropic distributions is 70.71%, and in our the samples is 71.44%, 62.62% and 72.35% for R, P and P.NB samples, respectively. At short distances ($r < 50$ kpc), satellites in P.NB systems have a small percentage of polar orbits (15.28%), while R systems have a larger percentage of polar orbit (84.95%) than in isotropic distributions. These results on R systems nicely agree with the 3D orbital structure of the Milky Way and M31 satellite systems (see §1). Another important result on orbital structure is that there are less retrograde orbits, in agreement with observational findings (Herbert-Fort et al. 2008).

As mentioned before, the fact that the trajectory of a satellite is polar at a given time does not imply that the satellite is within the polar cone at that time. As a matter of fact, satellites in our samples are more likely to be found in the equatorial region (70.86%, 71.34% and 67.58% for the R, P and P.NB samples, respectively), because the equatorial region occupies 70.71% of the sphere volume. Therefore it is not a simple task to infer 3D trajectories of satellites from their projected positions provided by observations (see §1). However, as explained above, our simulations allow us to mimic observations quite easily. As, in projection, disks identified in the

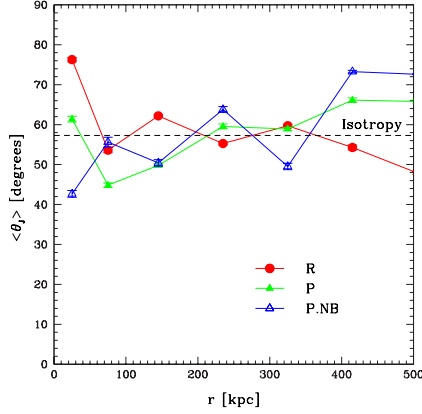


Fig.1 The average θ_J as a function of distance for the samples R, P and P.NB.

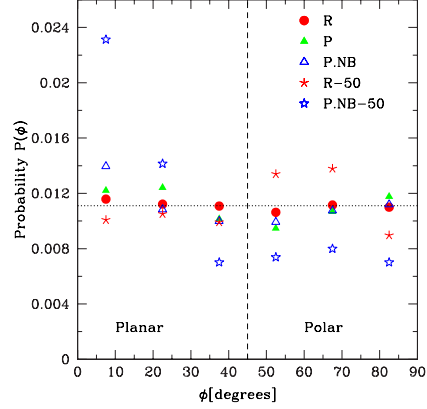


Fig.2 The probability distributions of the ϕ angles for satellites in the R, P, P.NB, R-50 and P.NB-50 samples. The dotted horizontal line represents an isotropic distribution.

simulations become ellipses, we can measure the angle ϕ between the major axis of these ellipses and the satellite projected position vector respect to the host, as done in observational analyses.

In Figure 2 we plot the probability distributions of ϕ , for the R, P and P.NB samples, compared with an isotropic distribution represented by the dotted horizontal line. Note that the R sample has an almost isotropic distribution, and the P and P.NB samples show a small excess of planar alignments. These findings compare satisfactorily well with observational analyses of large samples of isolated blue galaxies (see §1) or Brainerd's (2005) results. To deepen into these findings, we have studied the effects of the projected satellite-host distance d_p on the ϕ distribution. We show in the same figure the distribution of the R-50 and the P.NB-50 samples, which are subsamples of the R and P.NB samples, respectively, containing those satellites at projected distances $d_p < 50$ kpc from their host. The P.NB-50 sample presents a pronounced planar distribution, while the R-50 sample is rather polar. This increase in the fraction of planar alignments at low d_p is also reported by Brainerd (2005) for poor, isolated systems, while polar alignments at short projected distances are reported in rich systems (e.g., the Holmberg effect).

The behavior at short projected radial distances reflects the actual 3D orbital structure at short 3D distances (Figure 1), since the probability that an object at distance $r > 100$ kpc is observed with projected distance $d_p < 50$ kpc is very low¹ ($< 13.4\%$), therefore the alignments at $d_p < 50$ kpc virtually result only from the orbital structure at low r , and, as seen in Figure 1, at $r \leq 50$ kpc, the $\langle \theta_J \rangle$ values show polar distribution for the R sample, and non-polar for the P.NB sample.

¹ The probability that an object at distance $r = L$ of the host center-of-mass is seen under a random projection within a projected distance $d_p \leq l$ is given by the expression $P(x) = 1 - \sqrt{1 - x^2}$, with $x = l/L$

Results on orbit stability in disk-satellite systems from simulations with non-cosmological, predefined orbital initial conditions (Peñarrubia, Kroupa & Boily 2002) indicate that evolutive effects lead to a prevalence of polar orbits as compared with non-polar ones. This explains why in our disk-satellite systems polar orbits are more frequent, with possible contributions from satellite infall along filaments. The evolutive effects also explain the distance effect found in the 3D orbital structure of R and P samples. However, the trend towards an excess of non-polar orbits in PNB systems at short distances ($r \leq 50$ kpc) cannot be explained in terms of evolutive effects, but as a consequence of the assembly history of these isolated, poor systems. Our simulations indicate that these systems are formed in lower density and dynamically less active environments than populated systems, where gas acquisition forming the disk and satellite capture go together, so satellites follow gas structure.

In conclusion, we see that an almost isotropic distribution in 3D is consistent, when seen in projection, with a slightly polar alignment at short distances, with a planar alignment, or even with a lack of significant alignment, depending on the selection criteria used to build up the subsamples (as Bailin et al. 2007 have found in their analyses of the SDSS DR5 host-satellite systems). Our results can explain at the same time the 3D distribution of the Milky Way or M31 satellites in Great Circles roughly perpendicular to their disks (similar to the effect first detected by Holmberg in disk galaxies with a high number of satellites), and the planar alignments detected in projection in large redshift surveys when the systems are isolated and have a low number of satellites per host.

References

1. Agustsson, I., & Brainerd, T. 2006 *ApJ* **650**, 550
2. Azzaro, M., Patiri, S.G., Prada, F., & Zetner, A.R. 2007 *ApJ* **376**, L43
3. Bailin, J., Power, C., Norberg, P., Zaritsky, D., & Gibson, B.K. 2007, preprint (arXiv:0706.1350)
4. Brainerd, T.G. 2005 *ApJ* **628**, L101
5. Herbert-Fort, S., Zaritsky, D., Kim, Y.J., Bailin, J., & Taylor, J.E. 2008 *MNRAS* **384**, 803
6. Holmberg, E. 1969 *Ark. Astr* **5** 305
7. Kang X., Mao, S., Gao, L., & Jing, Y.P. 2005 *A&A* **437** 383
8. Koch, A. & Grebel, E.K. 2006 *AJ* **131**, 1405
9. Kroupa, P., Theis, C., & Boily, C.M. 2005 *A&A* **431**, 517
10. Libeskind, N.I., Frenk, C.S., Cole, S., Helly, J.C., Jenkins, A., Navarro, J.F., & Power, C. 2005 *MNRAS* **363**, 146
11. Libeskind, N.I., Cole, S., Frenk, C.S., Okamoto, T., & Jenkins, A. 2007 *MNRAS* **374**, 16
12. Lynden-Bell, D. 1982 *Obs* **102**, 202
13. Majewski, S. R. 1994 *ApJ* **431**, L17
14. Peñarrubia, J., Kroupa, P., & Boily, C.M., 2002 *MNRAS* **333**, 779
15. Sales, L.V., Navarro, J.F., Lambas, D.G., White, S.D.M., & Croton, D.J. 2007 *MNRAS* **382**, 1901
16. Sáiz, A., Domínguez-Tenreiro, R., Tissera, P.B., & Courteau, S. 2001 *MNRAS* **325**, 119
17. Serna, A., Domínguez-Tenreiro, R., & Sáiz, A. 2003 *ApJ* **597**, 878
18. Valtonen, M.J., Teerikorpi, P., & Argue, A.N. 1978 *AJ* **83**, 135
19. Zaritsky, D., Smith, R., Frenk, C., & White, S.D.M. 1997 *ApJ* **478**, 39
20. Zentner A.R., Kravtsov A., Gnedin O.Y., & Klypin, A. 2005 *ApJ* **629**, 219